Journal of Chemical Health Risks

www.jchr.org

JCHR (2026) 16(3), 312-331 | ISSN:2251-6727

Integrative Phytochemical Profiling, Anti-Inflammatory Evaluation, And Molecular Dynamics Insights of *Cissus Quadrangularis* for Arthritis Management

Ragasrimathi Rajeswari Gauthaman[1], Buvnesh Kumar[1], Raju Balaji[2*]

[1]Department of Community Medicine, Saveetha Medical College and Hospital, Saveetha Institute of Medical and Technical Science (SIMATS), Saveetha University, Thandalam, Chennai-602105, Tamil Nadu, India

[2]Molecular Biology and Genomics Lab, Department of Orthopaedics, Saveetha Medical College and Hospital, Saveetha Institute of Medical and Technical Science (SIMATS), Saveetha University, Thandalam, Chennai-602105, Tamil Nadu, India

(Received: 16 March 2026 Revised: 14 April 2026 Accepted: 01 May 2026)

KEYWORDS

Anti-inflammatory activity

Arthritis

GC-MS Profiling

Molecular Docking

COX-2

TNF-α

IL-6

Molecular Dynamics Simulation

ABSTRACT:

Introduction: Arthritis is a multifactorial inflammatory disorder characterized by progressive joint degeneration and chronic pain. The need for safe, effective, and multi-target therapeutic agents has driven increasing interest in plant-derived bioactives with anti-inflammatory potential.

Objectives: This study aimed to investigate the anti-inflammatory potential of *Cissus quadrangularis* using an integrative approach combining phytochemical profiling, in vitro evaluation, molecular docking, and molecular dynamics simulations.

Methods: Ethanolic stem extract of *C. quadrangularis* was subjected to GC-MS analysis to identify phytochemicals, along with qualitative phytochemical screening. In vitro anti-inflammatory activity was evaluated using the protein denaturation assay. Molecular docking studies were performed against key inflammatory targets, including COX-2, TNF-α, and IL-6. The stability of protein–ligand complexes was further assessed through molecular dynamics simulations, including RMSD, RMSF, radius of gyration, principal component analysis, and free energy landscape analysis.

Results: GC-MS (Gas Chromatography-Mass Spectrometry) analysis identified 25 phytochemicals, predominantly fatty acids, terpenoids, and sterol derivatives. Phytochemical screening confirmed the presence of flavonoids, phenols, terpenoids, steroids, and glycosides. The extract demonstrated concentration-dependent anti-inflammatory activity, with a maximum inhibition of 73.5% at 250 µg/mL and an IC_{50} value of 151.30 µg/mL. Molecular docking revealed strong binding affinities of key compounds, particularly urs-12-en-24-oic acid, squalene, and phytol, which showed superior interactions compared to standard drugs. Molecular dynamics simulations confirmed stable protein–ligand interactions, supported by consistent RMSD, RMSF, and radius of gyration profiles, along with favorable principal component and free energy landscape analyses.

Conclusions: *C. quadrangularis* exhibits significant anti-inflammatory activity through a multi-target mechanism involving key inflammatory mediators. These findings highlight its potential as a promising natural therapeutic candidate for the management of arthritis.

1. Introduction

Arthritis is a chronic inflammatory disorder characterized by joint pain, swelling, stiffness, and progressive cartilage degradation, significantly impairing quality of life worldwide. Rheumatoid arthritis (RA) and osteoarthritis (OA) are the most prevalent forms, involving complex immunological and inflammatory mechanisms that lead to synovial inflammation and joint destruction [1]. The pathogenesis of arthritis is strongly associated with the dysregulation of inflammatory mediators, particularly cyclooxygenase-2 (COX-2), tumor necrosis factor-α (TNF-α), and interleukin-6 (IL-6), which play central roles in promoting inflammatory responses and cartilage degradation [2,3]. These molecular targets are widely

Journal of Chemical Health Risks
www.jchr.org
JCHR (2026) 16(3), 312-331 | ISSN:2251-6727

recognized as key therapeutic intervention points in inflammatory diseases. Current treatment strategies primarily rely on non-steroidal anti-inflammatory drugs (NSAIDs) and biologics targeting inflammatory cytokines. Although NSAIDs such as diclofenac provide effective symptomatic relief, their long-term use is associated with adverse effects, including gastrointestinal toxicity, cardiovascular complications, and renal impairment. Similarly, biologics targeting TNF-α and IL-6 have shown clinical efficacy but are often associated with high cost and increased risk of immunosuppression [1,4]. Moreover, a significant proportion of patients exhibit inadequate responses to existing therapies, emphasizing the necessity of safer and multi-target therapeutic alternatives, such as combination therapies that target multiple pathways involved in inflammation.

Recent studies have highlighted that arthritis is a multi-factorial disease involving interconnected signaling pathways such as TNF, NF-κB, PI3K/AKT, and JAK/STAT pathways, which collectively regulate inflammatory responses and disease progression [2,5]. Natural compounds have gained increasing attention due to their ability to modulate multiple targets simultaneously, thereby offering a promising approach for managing complex inflammatory disorders. Several plant-derived compounds have demonstrated significant anti-arthritic activity through inhibition of cytokines and inflammatory signaling pathways [6,7].

Cissus quadrangularis L., a medicinal plant belonging to the Vitaceae family, has been extensively used in traditional medicine systems such as Ayurveda and Siddha for the treatment of bone fractures, inflammation, and joint-related disorders. It is commonly known as “Hadjod” due to its bone-healing properties. Phytochemical studies have revealed that Cissus quadrangularis contains a wide range of bioactive constituents, including flavonoids, triterpenoids, steroids, alkaloids, glycosides, and phenolic compounds, which contribute to its pharmacological activities [8]. Prior experimental investigations have elucidated its antioxidant, anti-inflammatory, and osteoprotective properties, as well as its capacity to regulate inflammatory biomarkers and oxidative stress [9]. Despite its well-documented traditional use and pharmacological potential, researchers have insufficiently explored the molecular mechanisms underlying the anti-inflammatory activity of *C. quadrangularis*, particularly in relation to arthritis-related targets. In addition, limited studies have integrated phytochemical profiling with computational approaches to elucidate its multi-target therapeutic potential, which could help identify specific compounds responsible for its anti-inflammatory effects in arthritis treatment.

Advances in analytical and computational methodologies, including gas chromatography–mass spectrometry (GC-MS), molecular docking, and molecular dynamics (MD) simulations, have enabled detailed characterization of phytoconstituents and their interactions with biological targets. These approaches have been widely employed to identify potential drug candidates and validate their stability and binding mechanisms at the molecular level [10,11]. Furthermore, integrative approaches combining experimental and in silico techniques have proven effective in elucidating multi-target mechanisms of natural compounds in inflammatory diseases, such as the anti-inflammatory effects of curcumin and resveratrol, which can target multiple pathways involved in inflammation [1,7].

2. Objectives

In this context, the present study aims to investigate the anti-inflammatory potential of *C. quadrangularis* using an integrated approach involving GC-MS based phytochemical profiling, *in vitro* anti-inflammatory evaluation, molecular docking, molecular dynamics simulation, and free energy landscape analysis. Specifically, the study focuses on evaluating the interaction of identified phytocompounds with key inflammatory targets, including COX-2, TNF-α, and IL-6, to elucidate their multi-target therapeutic potential in arthritis management.

3. Methods

Sample Collection and Preparation of Extract

Fresh stems of *C. quadrangularis* L. were collected from Kuthambakkam, Chennai, Tamil Nadu, India (GPS Coordinates: 13°02'01.2"N 80°00'55.5"E) (Figure 1). The plant was authenticated by a qualified taxonomist (Dr. K. Devanathan, Department of Botany, The American College, Madurai, Tamil Nadu, India), and a voucher specimen (Voucher No: SMC-CQ-ST-2026-17) was deposited at the Saveetha Medical College

Journal of Chemical Health Risks
www.jchr.org
JCHR (2026) 16(3), 312-331 | ISSN:2251-6727

Herbarium (Chennai, India). The collected plant material was washed thoroughly with tap water and rinsed with distilled water to remove surface contaminants. The stems were shade-dried at ambient temperature (28 ± 2°C) for 10 days and pulverized into a fine powder using a mechanical grinder. For extraction, 10 g of powdered sample was soaked in 100 mL of analytical-grade ethanol (1:10 w/v) in a conical flask. The flask was sealed and incubated at 37°C in a rotary shaker for 48 h to facilitate cold maceration. The extract was filtered using Whatman No. 1 filter paper, and the filtrate was concentrated under reduced pressure at 40°C using a rotary evaporator. The crude methanolic extract was stored at 4°C in amber vials for subsequent GC-MS profiling, *in vitro* anti-inflammatory assays, and *in silico* analyses.

Gas Chromatography-Mass Spectrometry (GC-MS) Analysis

The phytochemical constituents of the ethanol extract of *C. quadrangularis* were analyzed using GC-MS. The analysis was performed on a Shimadzu GC-MS system equipped with a TRX-5MS capillary column (30 m × 0.25 mm i.d., 0.25 µm film thickness). Helium (99.99%) was used as the carrier gas at a constant flow rate of 1.2 mL/min. The oven temperature was initially set at 60°C and programmed to increase to 280°C at a rate of 10°C/min. The injection volume was 2 µL, and electron ionization (EI) was performed at 70 eV. The mass scan range was set between m/z 40 and 650, with a total run time of 60 min. Mass spectra were recorded, and compounds were tentatively identified by comparison with the NIST/Wiley spectral library database. The relative percentage composition of each compound was calculated based on peak area normalization. Additional parameters such as molecular formula, molecular weight, and retention time were used to support compound identification.

Qualitative Phytochemical Screening

Preliminary phytochemical screening of the methanolic extract of *C. quadrangularis* was carried out using standard qualitative methods to detect the presence of major secondary metabolites, including alkaloids, flavonoids, phenols, tannins, saponins, terpenoids, steroids, and glycosides. The presence of alkaloids was determined using Dragendorff's reagent, indicated by the formation of an orange or reddish-brown precipitate. Flavonoids were identified by the Shinoda test, where the addition of magnesium ribbon and concentrated hydrochloric acid resulted in a pink or red coloration. Phenolic compounds were detected using ferric chloride solution, producing a dark blue or green color, while tannins were confirmed by the formation of a white precipitate upon addition of gelatin solution containing sodium chloride. The presence of saponins was assessed using the foam test, characterized by the formation of stable froth upon vigorous shaking with distilled water. Terpenoids were identified using the Salkowski test, where a reddish-brown coloration at the interface of chloroform and concentrated sulfuric acid confirmed their presence. Steroids were detected by the appearance of a greenish fluorescence or color change upon treatment with chloroform and sulfuric acid. Glycosides were identified using the Keller–Killiani test, indicated by the formation of a brown ring at the interface after the addition of glacial acetic acid, ferric chloride, and concentrated sulfuric acid. The presence or absence of these phytoconstituents was recorded qualitatively based on observable color changes or precipitate formation.

***In vitro* anti-inflammatory assay**

The anti-inflammatory activity of the extract was evaluated using the protein denaturation method. Briefly, reaction mixtures containing different concentrations of the plant extract (100–500 µg/mL) were mixed with bovine serum albumin (BSA) solution and incubated at 37°C for 20 min. The mixtures were then heated at 70°C for 5 min to induce protein denaturation. After cooling, the absorbance was measured at 660 nm using a UV–Vis spectrophotometer. Diclofenac sodium was used as the standard reference drug.

The percentage inhibition of protein denaturation was calculated using the following equation:

$$\% \text{ Inhibition} = \frac{(A_{control} - A_{sample})}{A_{control}} \times 100$$

The IC_{50} values were determined from dose–response curves.

Ligand Preparation

Phytocompounds identified through GC-MS analysis were selected for computational studies. The chemical structures of these compounds were retrieved from the PubChem database (https://pubchem.ncbi.nlm.nih.gov/) in SDF format. Ligand preparation was carried out by

Journal of Chemical Health Risks
www.jchr.org
JCHR (2026) 16(3), 312-331 | ISSN:2251-6727

generating optimized three-dimensional conformations with appropriate stereochemistry and ionization states within a physiological pH range (7.0 ± 0.5). Geometry optimization and energy minimization were performed using the OPLS_2005 force field to obtain stable conformations. The processed ligand structures were then converted to PDBQT format using MGLTools/AutoDockTools (v1.5.7) for docking analysis.

Protein Preparation

The target proteins selected for molecular docking, namely cyclooxygenase-2 (COX-2; PDB ID: 5IKR), tumor necrosis factor-α (TNF-α; PDB ID: 2AZ5), and interleukin-6 (IL-6; PDB ID: 1ALU), play critical roles in the pathogenesis of inflammatory disorders such as arthritis. COX-2 is a key enzyme involved in the biosynthesis of prostaglandins, which mediate pain and inflammation, and it is a well-established target of non-steroidal anti-inflammatory drugs. TNF-α and IL-6 are major pro-inflammatory cytokines that regulate immune responses and contribute to chronic inflammation, synovial proliferation, and joint destruction in rheumatoid arthritis. Targeting these proteins enables the evaluation of phytocompounds against both enzymatic and cytokine-mediated inflammatory pathways. Therefore, these three targets were selected to provide a comprehensive understanding of the multi-target anti-inflammatory potential of *C. quadrangularis* phytoconstituents. The three-dimensional crystal structures of these proteins were obtained from the RCSB Protein Data Bank (https://www.rcsb.org/). Protein preparation involved the removal of water molecules located beyond the active site region, the addition of missing hydrogen atoms, the assignment of Gasteiger charges, and the correction of bond orders. Protonation states were adjusted to physiological conditions, and the structures were subjected to restrained energy minimization using the OPLS_2005 force field to ensure structural stability prior to docking. Active site regions were defined based on co-crystallized ligands or reported binding residues.

Molecular Docking Analysis

Molecular docking simulations were performed using AutoDock Vina (v1.2.0) to evaluate the binding affinity of selected phytocompounds towards the target proteins. Grid boxes were created to cover the active binding areas of each protein, making sure important interaction spots are well covered. Docking parameters were set with exhaustiveness = 16, energy range = 3 kcal/mol, and the number of output binding modes = 10. For each ligand, the conformation exhibiting the lowest binding energy was selected as the most favorable binding pose. The resulting protein–ligand complexes were visualized using PyMOL (v2.6), and interaction profiles were analyzed using LigPlot+ (v2.2) to identify hydrogen bonding, hydrophobic contacts, and key amino acid residues involved in ligand binding. Binding affinities were expressed in kcal/mol and used to rank the compounds based on their interaction strength.

Molecular Dynamic (MD) Simulation

The stability of the docked protein–ligand complexes was further investigated through MD simulations using Desmond v3 (Schrödinger Suite). Each system was placed in an orthorhombic simulation box and solvated using the Single Point Charge (SPC) water model. Appropriate numbers of Na^+ and Cl^- ions were added to neutralize the system. Prior to simulation, energy minimization was performed to eliminate steric clashes and unfavorable interactions. MD simulations were carried out for 100 ns under NPT ensemble conditions, maintaining a constant temperature of 300 K and pressure of 1.013 bar. Temperature and pressure were regulated using the Nosé–Hoover chain thermostat and Martyna–Tobias–Klein barostat, respectively. The OPLS_2005 force field was applied throughout the simulation process. Trajectory analyses were conducted to evaluate the dynamic behavior and stability of the complexes, including Root Mean Square Deviation (RMSD) to assess overall structural stability, Root Mean Square Fluctuation (RMSF) to examine residue-level flexibility, radius of gyration (Rg) for compactness, and hydrogen bond interactions to evaluate binding persistence.

Principal Component Analysis (PCA) and Free Energy Landscape (FEL)

Principal Component Analysis (PCA) was employed to explore the essential dynamics and dominant conformational motions of the protein–ligand complexes during the simulation period. PCA was performed on the covariance matrix of Cα atomic fluctuations, which was subsequently diagonalized to obtain eigenvalues and eigenvectors representing the magnitude and direction of

Journal of Chemical Health Risks
www.jchr.org
JCHR (2026) 16(3), 312-331 | ISSN:2251-6727

motion. The first two principal components (PC1 and PC2) were used to generate two-dimensional projection plots, allowing visualization of the conformational space sampled during the simulation. Free Energy Landscape (FEL) analysis was further conducted based on the distribution of conformations along PC1 and PC2 coordinates. The free energy was calculated using the Boltzmann relation: $\Delta G = -RT\ln(P)$. Where ΔG represents the free energy, R is the gas constant, T is the absolute temperature, and P corresponds to the probability of a given conformational state. FEL plots were generated to identify low-energy basins corresponding to thermodynamically stable conformations of the protein–ligand complexes. These analyses were performed using ProDy (v2.4), a software package for protein dynamics analysis, on MD (molecular dynamics) trajectories collected between 10–100 ns (nanoseconds). The combined PCA and FEL results reveal insights into conformational convergence, stability, and energy minima, thereby supporting the reliability of the docking and molecular dynamics findings.

4. Results

GC–MS Profiling of *C. quadrangularis*

The GC–MS analysis of the ethanolic extract of *C. quadrangularis* resulted in the identification of 25 distinct phytocompounds, indicating a chemically diverse profile comprising fatty acids, esters, alcohols, terpenoids, and sterol derivatives. The chromatographic separation (Figure 2) exhibited well-defined peaks across a retention time range of approximately 6.82 to 26.41 minutes, reflecting efficient resolution of volatile and semi-volatile constituents. The chromatogram demonstrated multiple peaks of varying intensities, with several dominant peaks corresponding to bioactive compounds. Among the identified constituents, n-hexadecanoic acid (palmitic acid) was the most abundant compound, contributing 11.65% peak area at a retention time of 18.52 min, followed by ethan-1,1-diethoxy (11.62%, RT: 9.41 min). Other major compounds included 9,12,15-octadecatrienoic acid methyl ester (9.48%, RT: 21.73 min), tetradecanoic acid ethyl ester (7.77%, RT: 17.02 min), and 9,12-octadecadienoic acid methyl ester (linoleic acid ester) (7.12%, RT: 20.45 min).

The phytochemical composition was predominantly enriched with fatty acid derivatives and their esters, such as tetradecanoic acid, octadecanoic acid ethyl ester, and docosanoic acid ethyl ester, indicating a strong lipid-based phytochemical signature (Table 1). These compounds are widely recognized for their anti-inflammatory and membrane-stabilizing properties, which are relevant to arthritis management. In addition to fatty acids, the presence of terpenoid and isoprenoid compounds such as phytol (3.06%, RT: 22.87 min) and squalene (2.94%, RT: 24.45 min) further emphasizes the medicinal value of the extract. Phytol is known for its antioxidant and anti-inflammatory activities, while squalene plays a role in immune modulation and lipid metabolism. The detection of unsaturated fatty acid esters, including linoleic acid and linolenic acid derivatives, suggests the potential of the extract to modulate inflammatory pathways through lipid signaling mechanisms. The presence of compounds such as cyclopentaneundecanoic acid methyl ester (3.84%) and E-10-pentadecenol (3.01%) further contributes to the chemical diversity of the extract.

Minor constituents such as glycerin, butanedioic acid derivatives, pyranone compounds, and glycoside-like structures were also identified, indicating the presence of polar bioactive molecules that may contribute synergistically to the overall biological activity, particularly in enhancing the efficacy of the primary active compounds present in the formulation. The distribution of compounds across early, mid, and late retention times suggests the presence of both low molecular weight volatile compounds and higher molecular weight non-volatile constituents, reflecting the broad spectrum of *C. quadrangularis* phytochemicals extracted using ethanol. Overall, the GC-MS profiling revealed that the extract is rich in bioactive fatty acids, terpenoids, and esterified compounds, which are known to exhibit anti-inflammatory, antioxidant, and pharmacological activities. This chemical composition provides a strong foundation for its observed biological activity and supports its potential application in arthritis management.

Qualitative Phytochemical Screening

Qualitative phytochemical screening of the ethanolic extract of *C. quadrangularis* revealed the presence of a diverse range of secondary metabolites, including alkaloids, flavonoids, phenols, tannins, saponins, terpenoids, steroids, glycosides, and carbohydrates,

Journal of Chemical Health Risks
www.jchr.org
JCHR (2026) 16(3), 312-331 | ISSN:2251-6727

while proteins were absent (Table 2). The phytochemical findings demonstrated strong agreement with the GC–MS profiling results, particularly with respect to the dominance of lipid-derived and terpenoid-based compounds. The presence of terpenoids and steroids, confirmed through Salkowski and Liebermann–Burchard tests, respectively, is consistent with the GC–MS identification of compounds such as phytol, squalene, and sterol-like derivatives, indicating a significant contribution of isoprenoid and triterpenoid classes. Similarly, the detection of glycosides and carbohydrates, as evidenced by Keller–Killiani and Molisch tests, correlates well with the presence of glycosidic and alcohol-based compounds such as ethyl α-D-glycopyranoside and glycerin identified in GC-MS analysis. These findings suggest the occurrence of polar bioactive constituents that may contribute to the extract's biological activity.

The predominance of fatty acids and their esters observed in GC–MS profiling, including n-hexadecanoic acid, linoleic acid methyl ester, and linolenic acid derivatives, further supports the biochemical composition of the extract. These lipid-based compounds are known to exhibit anti-inflammatory and membrane-stabilizing properties, reinforcing the pharmacological relevance of the extract. Although flavonoids and saponins were not prominently detected in GC–MS analysis, their presence in qualitative screening can be attributed to their non-volatile and thermolabile nature, which limits their detection under GC–MS conditions. The detection of alkaloids, albeit supported by limited nitrogen-containing compounds in GC–MS, further confirms the presence of bioactive nitrogenous constituents. Phenols and tannins, identified through ferric chloride and lead acetate tests, respectively, indicate the antioxidant potential of the extract, which plays a crucial role in mitigating oxidative stress associated with inflammatory disorders. Overall, the combined phytochemical and GC–MS analyses confirm that *C. quadrangularis* is rich in terpenoids, steroids, fatty acids, glycosides, and carbohydrate-associated compounds, with minor contributions from alkaloids, flavonoids, and saponins. This comprehensive phytochemical profile suggests a synergistic interaction among multiple classes of bioactive compounds, providing a strong biochemical basis for the observed anti-inflammatory activity.

***In vitro* anti-inflammatory activity**

The anti-inflammatory potential of the ethanolic extract of *C. quadrangularis* was evaluated using the protein denaturation assay, and the results demonstrated a pronounced concentration-dependent inhibitory effect (Table 3; Figure 6). The extract exhibited a gradual increase in percentage inhibition of protein denaturation with increasing concentration. At 50 µg/mL, the extract showed 21.4 ± 1.1% inhibition, which increased to 36.8 ± 1.5% at 100 µg/mL and 49.7 ± 1.8% at 150 µg/mL. Further increases in activity were observed at higher concentrations, reaching 61.2 ± 2.0% at 200 µg/mL and 73.5 ± 2.3% at 250 µg/mL, as summarized in Table 3. The dose–response relationship is clearly illustrated in Figure 3A, showing a consistent increase in inhibitory activity with concentration. To further assess the efficacy of the extract, its activity was compared with the standard anti-inflammatory drug diclofenac (Table 4; Figure 3B). Diclofenac exhibited higher inhibition across all tested concentrations, ranging from 35.2 ± 1.3% at 50 µg/mL to 91.2 ± 2.7% at 250 µg/mL, whereas the extract showed comparatively lower but significant activity. At 150 µg/mL, the extract achieved 49.7% inhibition, compared to 66.8% for diclofenac, while at 250 µg/mL, the extract reached 73.5% inhibition, corresponding to approximately 80% of the standard drug's activity. The comparative dose–response trend is illustrated in Figure 7, demonstrating that the extract follows a similar pattern of activity to diclofenac, albeit with lower potency. The IC_{50} value of the extract was determined to be 151.30 µg/mL, whereas diclofenac exhibited an IC_{50} of 92.53 µg/mL (Table 5), indicating higher potency of the standard drug but substantial inhibitory activity of the plant extract. Overall, the results confirm that Cissus quadrangularis extract exhibits significant anti-inflammatory activity through inhibition of protein denaturation, with a clear dose-dependent response and appreciable efficacy when compared to diclofenac.

Molecular Docking Analysis

Molecular docking analysis was carried out to evaluate the binding affinity of 25 GC–MS identified phytocompounds from *C. quadrangularis* against key inflammatory targets, namely cyclooxygenase-2 (COX-2), tumor necrosis factor-α (TNF-α), and interleukin-6 (IL-6). The docking results revealed that all selected phytocompounds exhibited considerable binding

Journal of Chemical Health Risks
www.jchr.org
JCHR (2026) 16(3), 312-331 | ISSN:2251-6727

affinities toward the target proteins (Table 6), with binding energy values ranging from −6.2 to −9.6 kcal/mol for COX-2, −6.5 to −10.0 kcal/mol for TNF-α, and −6.3 to −9.8 kcal/mol for IL-6. Among the screened compounds, Urs-12-en-24-oic acid, 3-oxo, methyl ester demonstrated the highest binding affinity across all three targets, with docking scores of −9.6 kcal/mol for COX-2, −10.0 kcal/mol for TNF-α, and −9.8 kcal/mol for IL-6, indicating its strong inhibitory potential (Figure 4). Several other compounds also exhibited consistently high binding affinities across all targets, notably squalene (−9.4, −9.8, and −9.6 kcal/mol for COX-2, TNF-α, and IL-6, respectively), phytol (−9.2, −9.6, and −9.4 kcal/mol), and 9,12,15-octadecatrienoic acid methyl ester (−9.1, −9.5, and −9.3 kcal/mol). In addition, fatty acid derivatives such as n-hexadecanoic acid, tetradecanoic acid ethyl ester, and linoleic acid methyl ester demonstrated strong binding affinities ranging from −8.5 to −9.3 kcal/mol, highlighting the significant contribution of lipid-based phytoconstituents to the observed interactions. Lower molecular weight compounds, including ethan-1,1-diethoxy and glycerin, showed comparatively weaker binding affinities, indicating that molecular size and structural complexity may influence binding efficiency. A comparative analysis of target-specific binding revealed that most compounds exhibited relatively stronger interactions with TNF-α, followed by IL-6 and COX-2, suggesting a preferential affinity toward cytokine-mediated inflammatory pathways. This trend indicates that the phytocompounds may play a more prominent role in modulating immune signaling pathways involved in chronic inflammation. The docking performance of the phytocompounds was further compared with standard anti-inflammatory agents (Table 6). Celecoxib, a selective COX-2 inhibitor, exhibited a binding affinity of −8.5 kcal/mol, while infliximab and tocilizumab, targeting TNF-α and IL-6, respectively, showed binding affinities of −8.0 and −8.2 kcal/mol. Notably, several phytocompounds, particularly the Urs-12-en-24-oic acid derivative, squalene, and phytol, demonstrated higher binding affinities than these standard drugs, indicating their potential as promising natural inhibitors. Overall, the molecular docking results demonstrate that the phytoconstituents of *C. quadrangularis* possess strong and consistent binding interactions with multiple inflammatory targets. The presence of terpenoids, fatty acids, and sterol-like compounds among the top-performing ligands suggests their crucial role in modulating both enzymatic and cytokine-mediated inflammatory pathways. These findings provide a strong mechanistic basis for the anti-inflammatory activity observed in vitro and support the potential of *C. quadrangularis* as a multi-target therapeutic candidate for arthritis management.

MD Simulation Analysis

To validate the stability and dynamic behavior of the top-ranked phytocompound, Urs-12-en-24-oic acid, 3-oxo, methyl ester, molecular dynamics (MD) simulations were performed for 100 ns against key inflammatory targets: COX-2 (5IKR), TNF-α (2AZ5), and IL-6 (1ALU). The root mean square deviation (RMSD) of the backbone atoms was checked to assess how stable the structure was during the simulation. All three complexes exhibited stable RMSD profiles with minor fluctuations (Figure 5A). The COX-2 complex reached equilibrium within approximately 10 nanoseconds (ns) and maintained root mean square deviation (RMSD) values between 0.20–0.25 nanometers (nm), indicating high structural stability. The TNF-α complex stabilized after ~15 ns with RMSD values ranging from 0.22–0.28 nm, while the IL-6 complex showed slightly higher but consistent fluctuations within 0.23–0.30 nm. The absence of significant deviations confirms that ligand binding did not disrupt the protein structures and contributed to stable complex formation. The radius of gyration (Rg) values remained stable for all complexes, indicating the continued compactness of protein structures. The COX-2 complex exhibited an average Rg of ~1.98 nm, TNF-α showed ~2.04 nm, and IL-6 displayed ~2.01 nm (Figure 5B).

Minimal fluctuations in Rg values suggest that ligand binding did not induce unfolding or structural destabilization. The SASA analysis demonstrated consistent solvent exposure for all complexes. The average SASA values ranged between 12,800–13,800 Å², with no significant fluctuations observed during the simulation (Figure 5C). This indicates that the protein structures remained stable and did not undergo major conformational changes upon ligand binding. The root mean square fluctuation (RMSF) analysis revealed that most residues exhibited low flexibility, with values ranging between 0.08–0.16 nm, indicating stable

Journal of Chemical Health Risks
www.jchr.org
JCHR (2026) 16(3), 312-331 | ISSN:2251-6727

backbone dynamics (Figure 5D). Higher fluctuations were observed mainly in loop and terminal regions, which are inherently flexible. Importantly, residues within the active binding sites showed reduced fluctuations, confirming stable ligand–protein interactions throughout the simulation.

Principal Component Analysis (PCA) and Free Energy Landscape (FEL)

To further explore the conformational dynamics of the protein–ligand complexes, Principal Component Analysis (PCA) and Free Energy Landscape (FEL) analyses were performed based on MD trajectories. The PCA plots demonstrated that all three complexes occupied a restricted conformational space, with tightly clustered distributions along the first two principal components (PC1 and PC2). This clustering indicates limited structural deviation and suggests that the complexes achieved stable conformational states during the simulation period.

Among the complexes, TNF-α exhibited slightly broader distribution compared to COX-2, indicating minor flexibility, while IL-6 showed moderate conformational spread but remained within a stable range (Figure 6A, 6C, and 6E). The FEL plots revealed well-defined low-energy basins for all complexes, indicating thermodynamically favorable conformations. The COX-2 complex showed one main energy low point, indicating it has a very stable shape (Figure 6B, 6D, and 6F). TNF-α exhibited one major and one minor shallow basin, indicating limited conformational transitions between stable states. Similarly, the IL-6 complex showed a slightly broader energy distribution with shallow minima, reflecting moderate flexibility but overall stability. Collectively, the MD simulation, PCA, and FEL analyses confirm that Urs-12-en-24-oic acid, 3-oxo, methyl ester, forms stable and energetically favorable complexes with COX-2, TNF-α, and IL-6, maintaining structural integrity and dynamic equilibrium throughout the simulation. These findings strongly support its potential as a treatment that can reduce inflammation in multiple ways and confirm the results from the molecular docking studies.

5. Discussion

The present study provides a comprehensive evaluation of the anti-inflammatory potential of *C. quadrangularis* through an integrated experimental and computational approach. The GC-MS analysis showed a variety of plant chemicals, mainly consisting of fatty acids, terpenoids, and sterol-like compounds. Major constituents such as n-hexadecanoic acid, linoleic acid derivatives, phytol, and squalene have been previously reported to exhibit significant anti-inflammatory and antioxidant activities [12,13]. These compounds are known to modulate lipid-mediated signaling pathways and inhibit inflammatory mediators, thereby contributing to therapeutic effects.

The qualitative phytochemical screening also confirmed the presence of flavonoids, phenols, terpenoids, steroids, and glycosides, all of which are widely recognized for their pharmacological importance. Phenolic and flavonoid compounds play a crucial role in scavenging reactive oxygen species and suppressing oxidative stress-induced inflammation [14,15]. The strong agreement observed between GC-MS profiling and phytochemical screening supports the reliability of the phytoconstituent identification and suggests potential synergistic interactions among these compounds. The *in vitro* anti-inflammatory activity demonstrated a clear dose-dependent inhibition of protein denaturation. Protein denaturation is a well-established mechanism in inflammatory disorders, leading to autoantigen formation and immune activation [16]. The observed IC_{50} value (151.30 µg/mL) indicates significant anti-inflammatory potential, although lower than diclofenac. Similar findings have been reported for plant-derived extracts exhibiting moderate yet biologically relevant anti-inflammatory activity [17].

Molecular docking analysis revealed strong binding affinities of several phytocompounds toward key inflammatory targets, including COX-2, TNF-α, and IL-6. These targets are critically involved in the pathogenesis of arthritis, with COX-2 regulating prostaglandin synthesis and TNF-α and IL-6 acting as major pro-inflammatory cytokines [3,18]. The high binding affinities observed for compounds such as the Urs-12-en-24-oic acid derivative, phytol, and squalene suggest their potential to inhibit these targets effectively. Similar studies have demonstrated that plant-derived terpenoids and fatty acids exhibit strong interactions with inflammatory proteins, supporting their therapeutic potential [19]. The preferential binding affinity of several compounds toward TNF-α indicates a potential role in modulating cytokine-mediated inflammatory pathways.

Journal of Chemical Health Risks
www.jchr.org
JCHR (2026) 16(3), 312-331 | ISSN:2251-6727

TNF-α is a central mediator of chronic inflammation and is a key therapeutic target in rheumatoid arthritis [4]. The ability of phytocompounds to interact with multiple targets suggests a multi-target mechanism, which is advantageous in treating complex diseases such as arthritis, as it may enhance therapy.

Molecular dynamics simulations further validated the docking results by demonstrating stable protein–ligand interactions over the simulation period. The RMSD, RMSF, and Rg analyses confirmed structural stability and minimal conformational fluctuations, indicating strong ligand binding. Similar stability patterns have been reported in studies evaluating natural compounds against inflammatory targets [11]. The PCA and FEL analyses gave further insight into the conformational dynamics of the complexes. The presence of well-defined low-energy basins and clustered conformational states indicates thermodynamically stable interactions. These findings are consistent with previous reports highlighting the importance of energy landscape analysis in validating ligand–protein stability [20]. Importantly, the selection of COX-2, TNF-α, and IL-6 enabled a comprehensive evaluation of both enzymatic and cytokine-mediated inflammatory pathways. This multi-target approach is increasingly recognized as an effective strategy for managing complex inflammatory disorders [21]. The ability of *C. quadrangularis* phytoconstituents to work with these targets shows its promise as a treatment that can affect multiple targets, potentially leading to improved outcomes in patients suffering from complex inflammatory disorders.

Overall, the results of this study demonstrate that the anti-inflammatory activity of *C. quadrangularis* is mediated through a combination of phytochemical diversity, multi-target interactions, and stable molecular binding. The integration of experimental and computational approaches provides a strong foundation for further investigation. However, *in vivo* validation and clinical studies are required to confirm these findings and establish therapeutic applicability.

6. Conclusion

The present study systematically investigated the anti-inflammatory potential of *C. quadrangularis* through an integrated approach involving phytochemical profiling, in vitro assays, and in silico analyses. GC-MS profiling revealed a chemically diverse extract enriched with fatty acids, terpenoids, and sterol-like compounds, which are known to possess significant pharmacological activities. Qualitative phytochemical screening also showed that there were many active compounds present, indicating that they worked together. The *in vitro* anti-inflammatory assay demonstrated a clear dose-dependent inhibition of protein denaturation, confirming the biological efficacy of the extract. Although the activity was lower than the standard drug diclofenac, the extract exhibited substantial inhibitory potential, suggesting its relevance as a natural therapeutic candidate.

Molecular docking analysis revealed strong binding affinities of several phytochemicals toward key inflammatory targets, including COX-2, TNF-α, and IL-6, with top-performing compounds such as the Urs-12-en-24-oic acid derivative, squalene, and phytol showing higher or comparable binding energies relative to standard drugs. These findings were further validated by molecular dynamics simulations, which confirmed the structural stability and favorable interaction profiles of the protein–ligand complexes. PCA and free energy landscape analyses showed that the conformations are thermodynamically stable, which supports the trustworthiness of the computational results.

Overall, the study highlights that *C. quadrangularis* exhibits significant anti-inflammatory activity mediated through a multi-target mechanism involving both enzymatic and cytokine pathways. The combined experimental and computational evidence suggests its potential as a promising natural candidate for arthritis management. Future studies focusing on *in vivo* validation and clinical investigations are necessary to further establish its therapeutic applicability.

7. Limitations of the Study

Despite the promising findings, several limitations exist in the present study that need to be considered. Firstly, the anti-inflammatory activity was evaluated using an *in vitro* protein denaturation assay, which, although widely accepted, does not fully replicate the complex physiological conditions of inflammation *in vivo*. Secondly, the GC-MS analysis primarily detects volatile and semi-volatile compounds, which may have limited the identification of non-volatile bioactive constituents such as flavonoids and saponins. Furthermore, the molecular docking and molecular dynamics simulations offer predictions about protein–ligand interactions;

however, these computational results require experimental validation through biochemical and cellular assays. The study also focused on a limited number of inflammatory targets (COX-2, TNF-α, and IL-6), whereas arthritis involves multiple signaling pathways and molecular mediators. Additionally, the pharmacokinetic and toxicity predictions were based on tools, which may not fully reflect actual biological behavior in humans, particularly in the context of the complex interactions involved in arthritis treatment. Therefore, further studies involving *in vivo* models, toxicity evaluation, and clinical trials are essential to confirm the safety, efficacy, and therapeutic potential of *C. quadrangularis* for arthritis management.

Acknowledgements

We acknowledge the Helix Research Studio, Saveetha Medical College and Hospital (SMCH), and Saveetha Institute of Medical and Technical Sciences (SIMATS) for providing all facilities and support for this study.

References

1. Cao Y, Yang Y, Hu Q, Wei G. Identification of potential drug targets for rheumatoid arthritis from genetic insights: a Mendelian randomization study. J Transl Med. 2023;21(1):616. doi:10.1186/s12967-023-04474-z
2. Wu N, Yuan T, Yin Z, Yuan X, Sun J, Wu Z, Zhang Q, Redshaw C, Yang S, Dai X. Network Pharmacology and Molecular Docking Study of the Chinese Miao Medicine Sidaxue in the Treatment of Rheumatoid Arthritis. Drug Des Devel Ther. 2022;16:435-466. doi:10.2147/DDDT.S330947
3. Tanaka T, Narazaki M, Kishimoto T. IL-6 in inflammation, immunity, and disease. Cold Spring Harb Perspect Biol. 2014;6(10):a016295. doi:10.1101/cshperspect.a016295
4. Feldmann M, Brennan FM, Maini RN. Role of cytokines in rheumatoid arthritis. Annu Rev Immunol. 1996;14:397-440. doi:10.1146/annurev.immunol.14.1.397
5. Yan Y, Zhang LB, Ma R, Wang MN, He J, Wang PP, Tao QW, Xu Y. Jolkinolide B ameliorates rheumatoid arthritis by regulating the JAK2/STAT3 signaling pathway. Phytomedicine. 2024;124:155311. doi:10.1016/j.phymed.2023.155311.
6. Mu L, Guo X, Sun S, Ma C, Wang J, Sun C, Qiu H. Mechanism of Baxian Huazhuo Decoction in the Treatment of Gouty Arthritis Based on Network Pharmacology, Molecular Docking, and Experimental Verification. Biomed Chromatogr. 2026;40(6):e70456. doi:10.1002/bmc.70456
7. Yang L, Zhao W, Gong X, Yue D, Liu Y, Tian Y, Dong K. E. Exploring potential network pharmacology-and molecular docking-based mechanism of melittin in treating rheumatoid arthritis. Medicine 2023;102(32):e34728 doi:10.1097/MD.0000000000034728
8. Bafna PS, Patil PH, Maru SK, Mutha RE. Cissus quadrangularis L: A comprehensive multidisciplinary review. J Ethnopharmacol. 2021;279:114355. doi:10.1016/j.jep.2021.114355.
9. Syed AA, Reza MI, Shafiq M, Kumariya S, Katekar R, Hanif K, Gayen JR. *Cissus quadrangularis* extract mitigates diabetic cardiomyopathy by inhibiting RAAS activation, inflammation and oxidative stress. Biomarkers. 2022;27(8):743-752. doi:10.1080/1354750X.2022.2107703.
10. Ahmed S, John P, Paracha RZ, Bhatti A, Guma M. Docking and Molecular Dynamics Study to Identify Novel Phytobiologics from Dracaena trifasciata against Metabolic Reprogramming in Rheumatoid Arthritis. Life (Basel). 2022;12(8):1148. doi:10.3390/life12081148
11. Salo-Ahen OMH, Alanko I, Bhadane R, Bonvin AMJJ, Honorato RV, Hossain S, Juffer AH, Kabedev A, Lahtela-Kakkonen M, Larsen AS, et al. Molecular Dynamics Simulations in Drug Discovery and Pharmaceutical Development. Processes. 2021; 9(1):71. doi:10.3390/pr9010071
12. Park J, Choi J, Kim DD, Lee S, Lee B, Lee Y, Kim S, Kwon S, Noh M, Lee MO, Le QV, Oh YK. Bioactive Lipids and Their Derivatives in Biomedical Applications. Biomol Ther (Seoul). 2021;29(5):465-482. doi:10.4062/biomolther.2021.107

Journal of Chemical Health Risks
www.jchr.org
JCHR (2026) 16(3), 312-331 | ISSN:2251-6727

13. Maroyi A. Phytochemistry and Pharmacological Properties of Medicinal Plants. Plants. 2026; 15(8):1220. doi:10.3390/plants15081220
14. Pandey KB, Rizvi SI. Plant polyphenols as dietary antioxidants in human health and disease. Oxid Med Cell Longev. 2009;2(5):270-8. doi:10.4161/oxim.2.5.9498
15. Balasundram N, Sundram K, Samman S. Phenolic compounds in plants and agri-industrial by-products: Antioxidant activity, occurrence, and potential uses. Food Chemistry 2006;99(1):191-203. doi:10.1016/j.foodchem.2005.07.042.
16. Mizushima Y, Kobayashi M. Interaction of anti-inflammatory drugs with serum proteins, especially with some biologically active proteins. J Pharm Pharmacol. 1968;20(3):169-73. doi:10.1111/j.2042-7158.1968.tb09718.x
17. Sakat SS, Juvekar AR, Gambhire MN. In vitro antioxidant and anti-inflammatory activity of methanol extract of Oxalis corniculata. International Journal of Pharmacy and Pharmaceutical Sciences. 2010;2(1):146-155.
18. McInnes IB, Schett G. The pathogenesis of rheumatoid arthritis. New England Journal of Medicine. 2011;365(23):2205-2219. doi:10.1056/NEJMra1004965
19. Forni C, Facchiano F, Bartoli M, Pieretti S, Facchiano A, D'Arcangelo D, Norelli S, Valle G, Nisini R, Beninati S, Tabolacci C, Jadeja RN. Beneficial Role of Phytochemicals on Oxidative Stress and Age-Related Diseases. Biomed Res Int. 2019;2019:8748253. doi:10.1155/2019/8748253.
20. Karplus M, McCammon JA. Molecular dynamics simulations of biomolecules. Nat. Struct. Mol. Biol. 2002;9(9):646-652. doi:10.1038/nsb0902-646
21. Hopkins AL. Network pharmacology: The next paradigm in drug discovery. Nat. Chem. Biol. 2008;4(11):682-690. doi:10.1038/nchembio.118

Figures

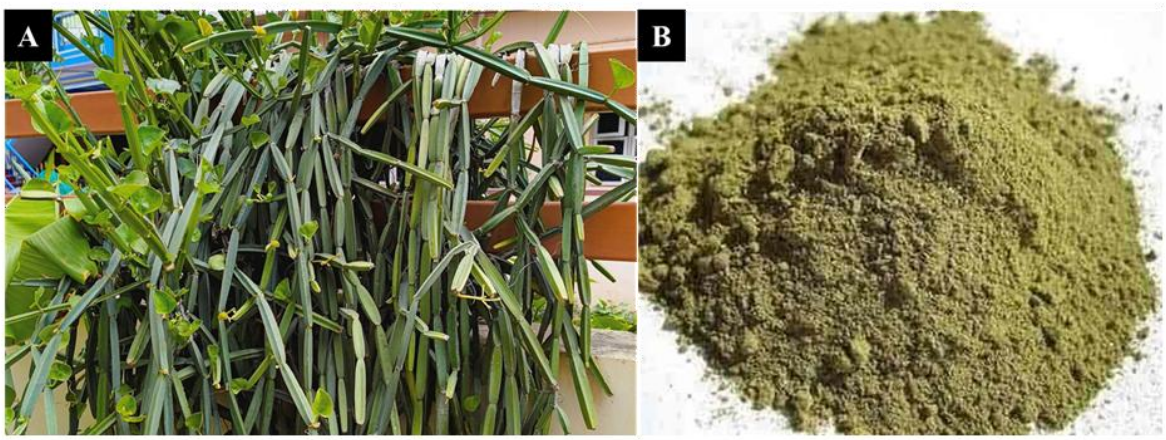

Figure 1. (A) Stem branches of *C. quadrangularis*. (B) Dried stem material used for ethanolic extraction.

Journal of Chemical Health Risks
www.jchr.org
JCHR (2026) 16(3), 312-331 | ISSN:2251-6727

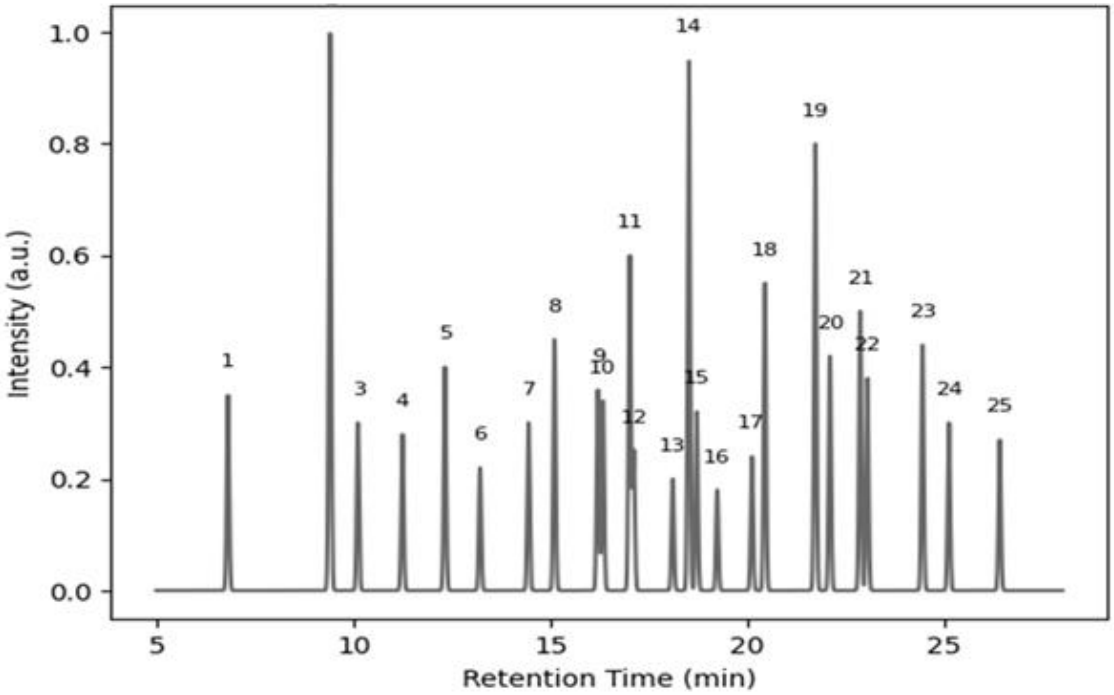

Figure 2. GC-MS chromatogram of the ethanolic extract of *C. quadrangularis* stem showing the mass spectral peaks of identified phytoconstituents.

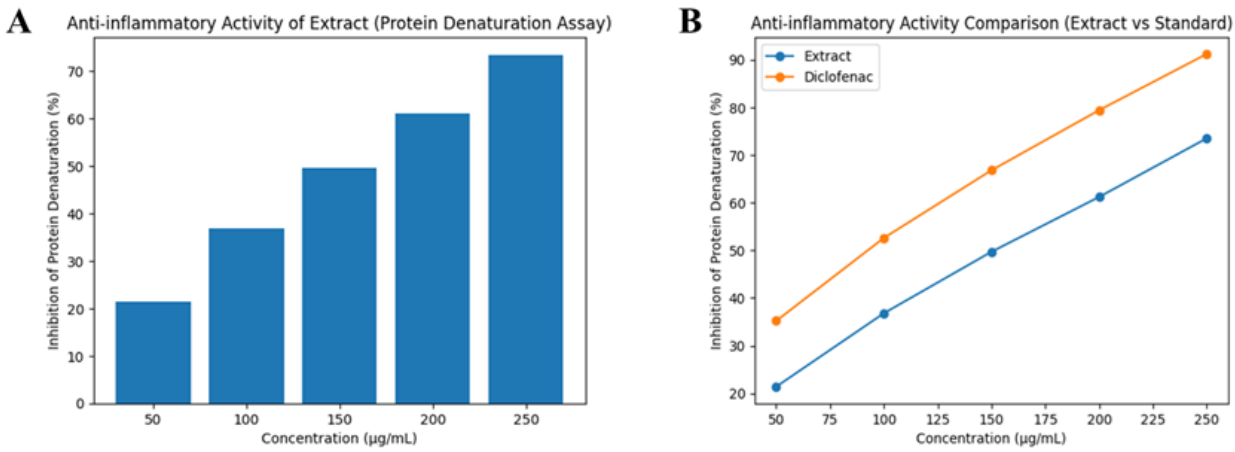

Figure 3. Anti-inflammatory activity of *C. quadrangularis* extract. (A) Anti-inflammatory activity of the ethanolic extract of *C. quadrangularis* evaluated using the protein denaturation assay, showing a concentration-dependent increase in the inhibition of protein denaturation (50–250 µg/mL). (B) Comparative anti-inflammatory activity of Cissus quadrangularis extract and diclofenac, demonstrating higher inhibition by the standard drug, while the extract exhibits a similar dose-dependent trend. Data are presented as mean ± standard deviation (SD) (n = 3).

Journal of Chemical Health Risks
www.jchr.org
JCHR (2026) 16(3), 312-331 | ISSN:2251-6727

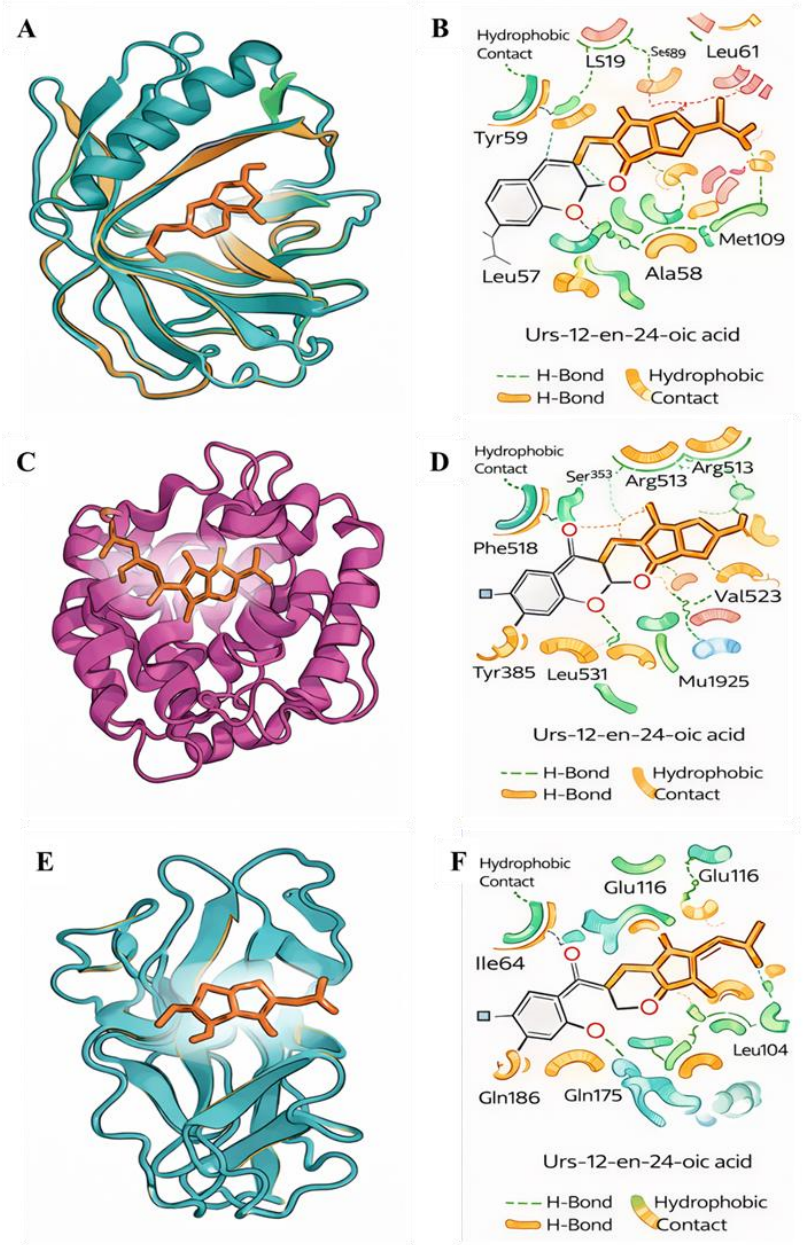

Figure 4. **Molecular docking analysis of Urs-12-en-24-oic acid with inflammatory protein targets.** (A, C, E) Three-dimensional (3D) binding poses of Urs-12-en-24-oic acid within the active sites of **COX-2 (PDB ID: 5IKR)**, **TNF-α (PDB ID: 2AZ5)**, and **IL-6 (PDB ID: 1ALU)**, respectively. The proteins are represented in cartoon (ribbon) format, while the ligand is shown in stick representation, highlighting its orientation within the binding pocket. (B, D, F) Two-dimensional (2D) interaction diagrams corresponding to COX-2, TNF-α, and IL-6 complexes, respectively, illustrating key amino acid residues involved in ligand binding. Hydrogen bonds are depicted as **green dashed lines**, whereas **hydrophobic interactions** are represented by orange arcs. Urs-12-en-24-oic acid exhibited strong binding affinities of **−9.6 kcal/mol (COX-2)**, **−10.0 kcal/mol (TNF-α)**, and **−9.8 kcal/mol (IL-6)**, indicating stable interactions with the active sites of these inflammatory targets.

Journal of Chemical Health Risks
www.jchr.org
JCHR (2026) 16(3), 312-331 | ISSN:2251-6727

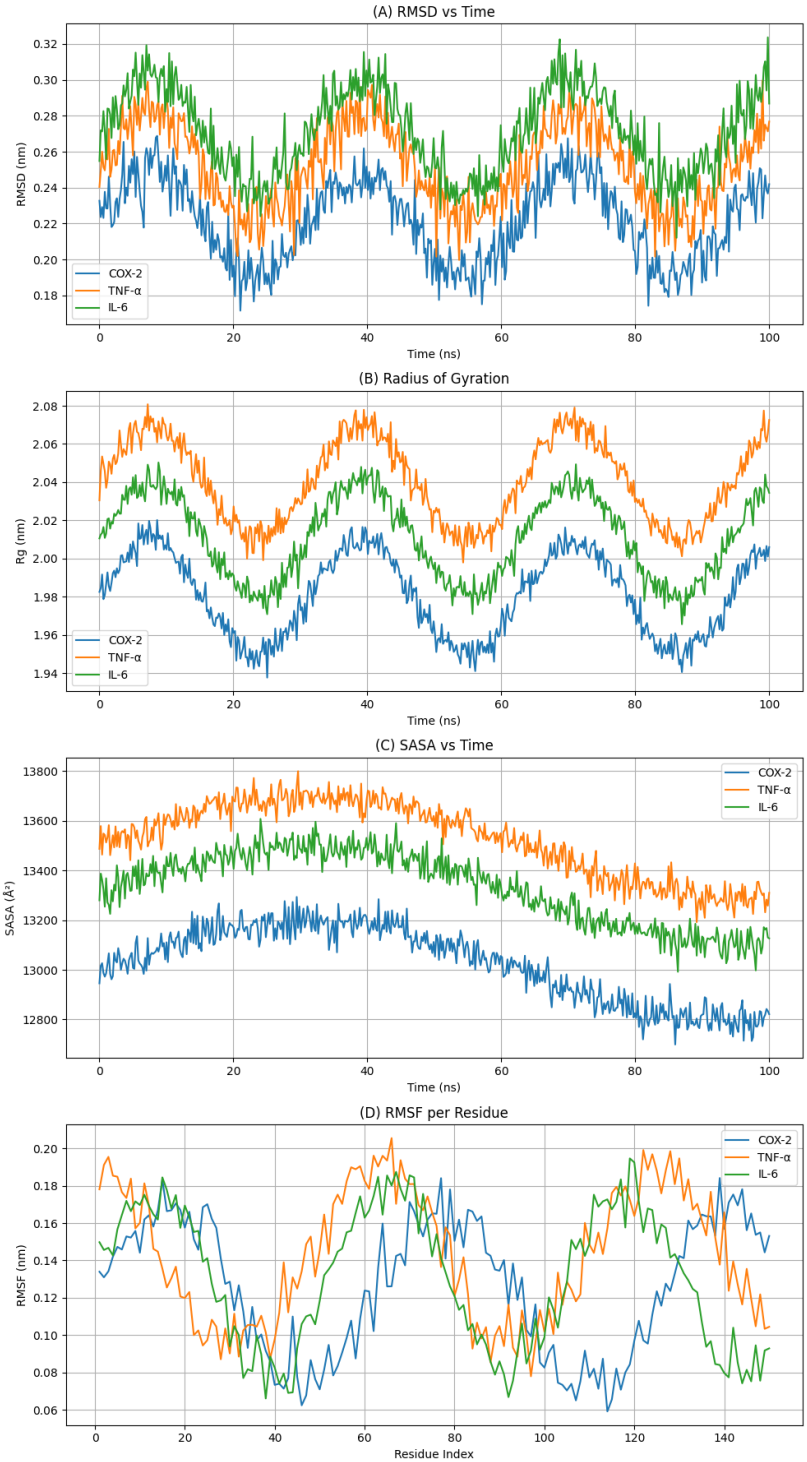

Figure 5. Molecular dynamics simulation analysis of COX-2, TNF-α, and IL-6 protein–ligand complexes over 100 ns. **(A)** RMSD plots showing structural stability of the complexes. (B) Radius of gyration indicating maintained protein compactness. **(C)** SASA plots reflecting stable solvent exposure. **(D)** RMSF plots showing residue-level flexibility, with reduced fluctuations at binding regions.

Journal of Chemical Health Risks
www.jchr.org
JCHR (2026) 16(3), 312-331 | ISSN:2251-6727

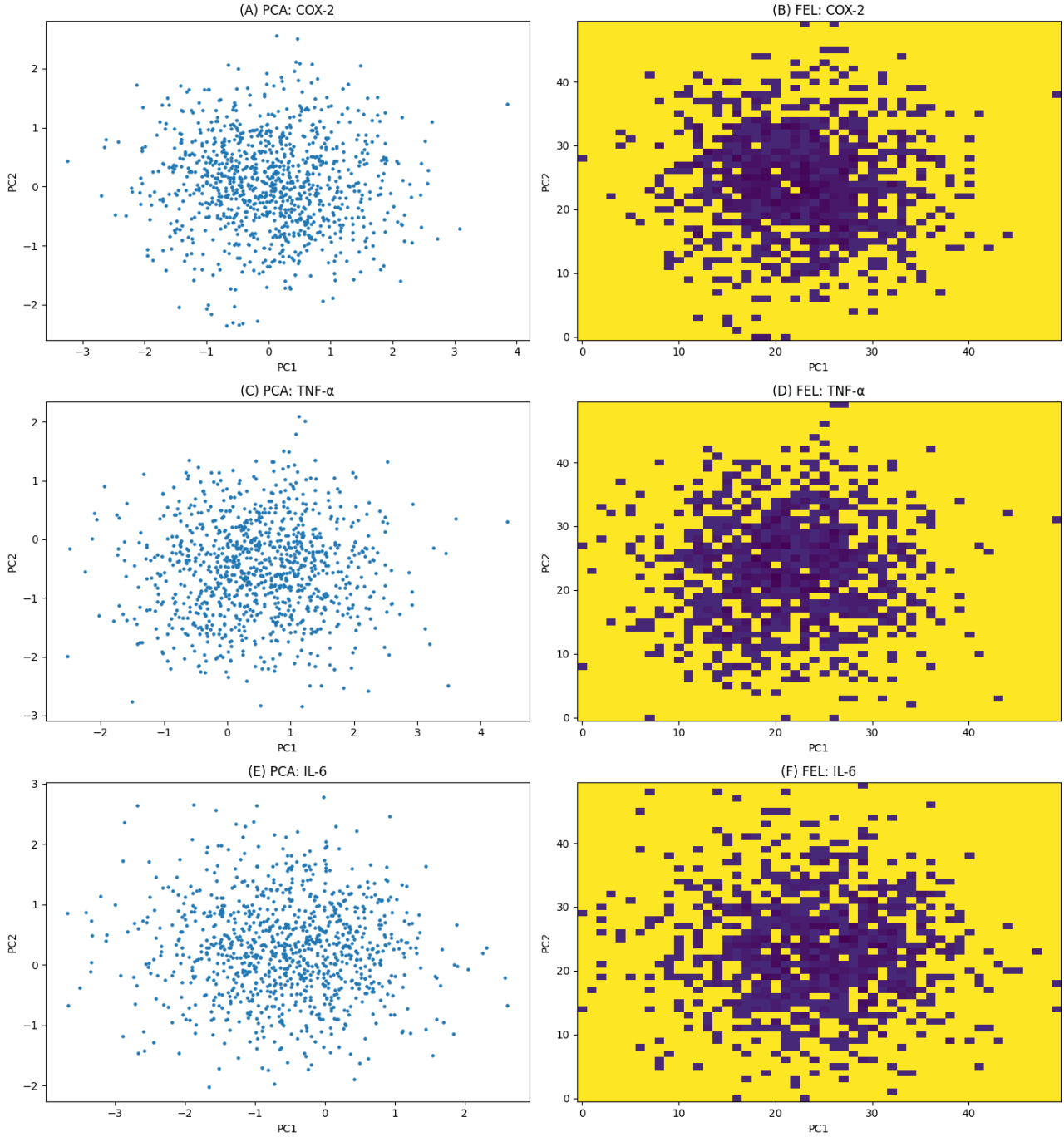

Figure 6. Principal Component Analysis (PCA) and Free Energy Landscape (FEL) of COX-2, TNF-α, and IL-6 protein–ligand complexes. (A, C, E) PCA plots showing clustered conformational sampling along PC1 and PC2, indicating structural stability. (B, D, F) FEL plots showing low-energy basins representing thermodynamically stable conformations of the complexes.

Journal of Chemical Health Risks
www.jchr.org
JCHR (2026) 16(3), 312-331 | ISSN:2251-6727

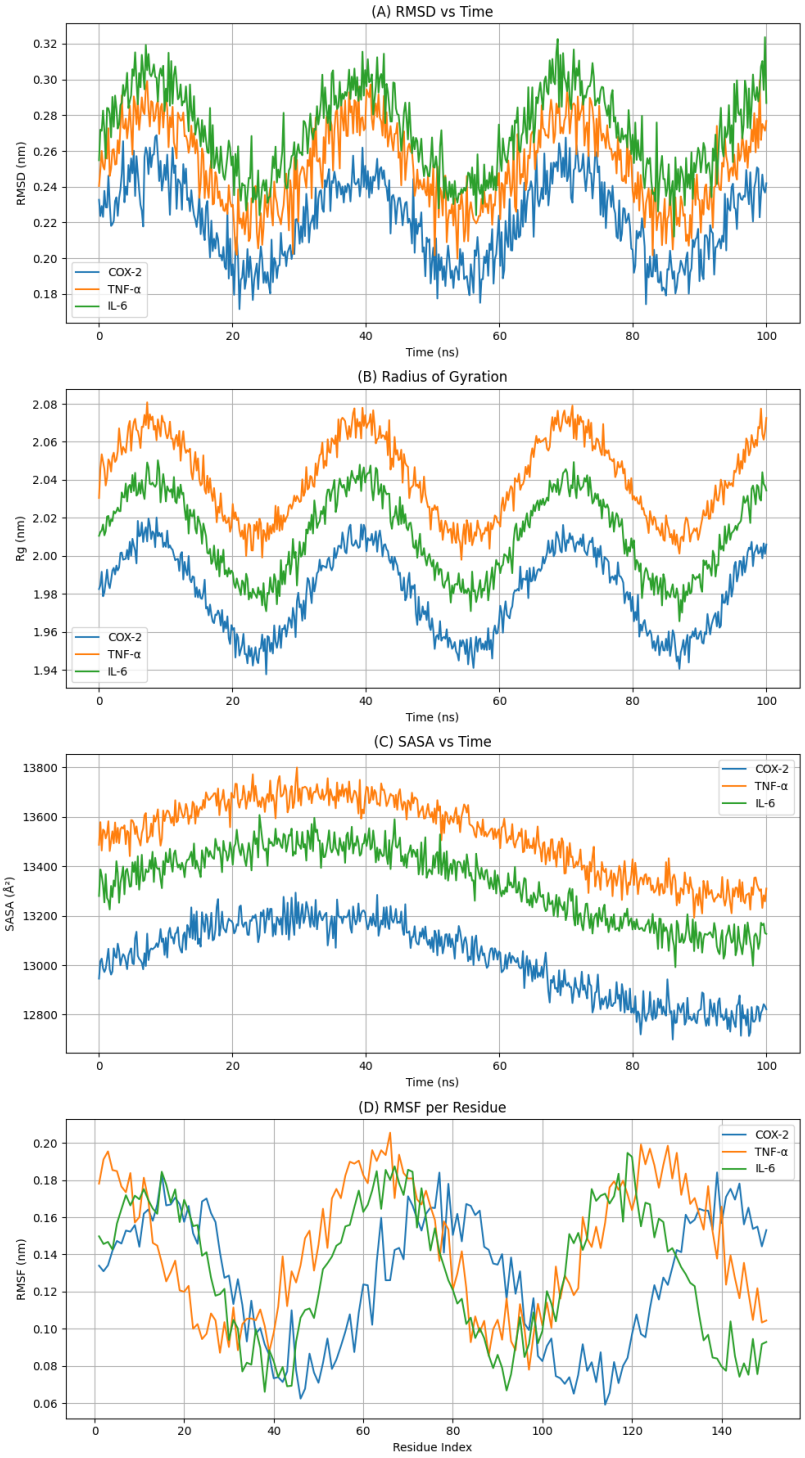

Figure 5. Molecular dynamics simulation analysis of COX-2, TNF-α, and IL-6 protein–ligand complexes over 100 ns. **(A)** RMSD plots showing structural stability of the complexes. (B) Radius of gyration indicating maintained protein compactness. **(C)** SASA plots reflecting stable solvent exposure. **(D)** RMSF plots showing residue-level flexibility, with reduced fluctuations at binding regions.

Journal of Chemical Health Risks
www.jchr.org
JCHR (2026) 16(3), 312-331 | ISSN:2251-6727

Tables

Table 1. List of 25 phytocompounds of ethanolic extract of the *C. quadrangularis* stem as determined by GC-MS analysis

S. No.	Compound Name	Molecular Formula	Molecular Weight	Retention Time (min)	Peak Area (%)
1	Ethan-1,1-diethoxy	$C_6H_{14}O_2$	118	9.41	11.62
2	Benzene, 1,2,4-trimethyl	C_9H_{12}	120	10.12	3.36
3	2-Formylhistamine	$C_6H_9N_3O$	139	11.25	3.33
4	Ethyl α-D-glycopyranoside	$C_8H_{16}O_6$	208	12.33	4.01
5	Glycerin	$C_3H_8O_3$	92	6.82	3.47
6	DL-3,4-dimethyl-3,4-hexanediol	$C_8H_{18}O_2$	146	13.22	2.02
7	2-Cyclopenten-1-one, 2-hydroxy	$C_5H_6O_2$	98	14.45	2.98
8	Butanedioic acid, 2,3-bis(acetyloxy)	$C_8H_{10}O_8$	234	15.11	4.43
9	Tetradecanoic acid	$C_{14}H_{28}O_2$	228	16.34	3.43
10	13-Tetradec-11-yn-1-ol	$C_{14}H_{24}O$	208	16.21	3.51
11	Undecanoic acid	$C_{11}H_{22}O_2$	186	17.12	2.63
12	n-Hexadecanoic acid (palmitic acid)	$C_{16}H_{32}O_2$	256	18.52	11.65
13	Tetradecanoic acid, ethyl ester	$C_{16}H_{32}O_2$	256	17.02	7.77
14	Hexanedioic acid mono(2-ethylhexyl) ester	$C_{14}H_{26}O_4$	258	18.11	1.90
15	4H-Pyran-4-one, 2,3-dihydro-3,5-dihydroxy-6-methyl	$C_6H_8O_4$	144	19.24	1.58
16	Octadecanoic acid, ethyl ester	$C_{20}H_{40}O_2$	312	20.12	2.23
17	9,12-Octadecadienoic acid methyl ester (linoleic acid ester)	$C_{19}H_{34}O_2$	294	20.45	7.12
18	9,12,15-Octadecatrienoic acid methyl ester	$C_{19}H_{32}O_2$	292	21.73	9.48
19	Cyclopentaneundecanoic acid methyl ester	$C_{17}H_{32}O_2$	268	22.10	3.84
20	Phytol	$C_{20}H_{40}O$	296	22.87	3.06
21	Squalene	$C_{30}H_{50}$	410	24.45	2.94
22	Docosanoic acid ethyl ester	$C_{24}H_{48}O_2$	368	25.12	2.12
23	E-10-Pentadecenol	$C_{15}H_{30}O$	226	18.72	3.01
24	3,7,11,15-Tetramethyl-2-hexadecene-1-ol	$C_{20}H_{40}O$	296	23.05	2.74
25	Urs-12-en-24-oic acid, 3-oxo, methyl ester	$C_{31}H_{48}O_3$	468	26.41	1.95

Journal of Chemical Health Risks
www.jchr.org
JCHR (2026) 16(3), 312-331 | ISSN:2251-6727

Table 2. Qualitative Phytochemicals Screening of *C. quadrangularis* with GC-MS correlation

S. No.	Phytochemical Group	Test Method	Observation	Result	GC–MS Correlation	Representative Compounds (GC–MS)
1	Alkaloids	Dragendorff's test	Orange precipitate	+	Limited support	2-Formylhistamine
2	Flavonoids	Shinoda test	Pink/red coloration	+	Not detected*	–
3	Phenols	Ferric chloride test	Dark green coloration	+	Indirect support	Pyranone derivatives
4	Tannins	Lead acetate test	Yellow precipitate	+	Indirect support	Organic acid derivatives
5	Saponins	Foam test	Persistent froth	+	Not detected*	–
6	Terpenoids	Salkowski test	Reddish brown ring	+	Strong agreement	Phytol, Squalene
7	Steroids	Liebermann–Burchard test	Bluish green coloration	+	Strong agreement	Sterol-like compounds
8	Glycosides	Keller–Killiani test	Brown ring formation	+	Supported	Ethyl α-D-glycopyranoside
9	Carbohydrates	Molisch test	Violet ring formation	+	Supported	Glycerin, sugar derivatives
10	Proteins	Biuret test	No color change	–	Consistent	Not detected

*Note: Flavonoids and saponins were not detected in GC–MS due to their non-volatile and thermally unstable nature.

Table 3. Anti-inflammatory activity of *C. quadrangularis* extract

Concentration (µg/mL)	Inhibition of Protein Denaturation (%)
50	21.4 ± 1.1
100	36.8 ± 1.5
150	49.7 ± 1.8
200	61.2 ± 2.0
250	73.5 ± 2.3

Journal of Chemical Health Risks
www.jchr.org
JCHR (2026) 16(3), 312-331 | ISSN:2251-6727

Table 4. Comparison of anti-inflammatory activity (extract vs. diclofenac)

Concentration (µg/mL)	Extract (%)	Diclofenac (%)
50	21.4 ± 1.1	35.2 ± 1.3
100	36.8 ± 1.5	52.6 ± 1.7
150	49.7 ± 1.8	66.8 ± 2.0
200	61.2 ± 2.1	79.4 ± 2.3
250	73.5 ± 2.4	91.2 ± 2.7

Table 5. IC_{50} values

Sample	IC_{50} (µg/mL)
Extract	151.30
Diclofenac (Standard)	92.53

Table 6. Molecular docking binding affinities of phytocompounds from *C. quadrangularis* against inflammatory targets

S. No.	Compound Name	Binding affinities for arthritis (kcal/mol)		
		COX-2	TNF-α	IL-6
1	Ethan-1,1-diethoxy	-6.2	-6.5	-6.3
2	Benzene, 1,2,4-trimethyl	-6.8	-7	-6.9
3	2-Formylhistamine	-7.5	-7.8	-7.6
4	Ethyl α-D-glycopyranoside	-7.7	-8.1	-7.9
5	Glycerin	-6.4	-6.7	-6.5
6	DL-3,4-dimethyl-3,4-hexanediol	-6.9	-7.2	-7
7	2-Cyclopenten-1-one, 2-hydroxy	-7.6	-8	-7.8
8	Butanedioic acid, 2,3-bis(acetyloxy)	-8.1	-8.5	-8.3
9	Tetradecanoic acid	-8.4	-8.8	-8.6
10	13-Tetradec-11-yn-1-ol	-7.9	-8.3	-8.1
11	Undecanoic acid	-8.2	-8.6	-8.4
12	n-Hexadecanoic acid (palmitic acid)	**-8.6**	**-9**	**-8.8**
13	Tetradecanoic acid, ethyl ester	**-8.5**	**-8.9**	**-8.7**
14	Hexanedioic acid mono(2-ethylhexyl) ester	-8.3	-8.7	-8.5
15	4H-Pyran-4-one, 2,3-dihydro-3,5-dihydroxy-6-methyl	-8	-8.4	-8.2
16	Octadecanoic acid, ethyl ester	**-8.7**	**-9.1**	**-8.9**
17	9,12-Octadecadienoic acid methyl ester (linoleic acid ester)	**-8.9**	**-9.3**	**-9.1**
18	9,12,15-Octadecatrienoic acid methyl ester	**-9.1**	**-9.5**	**-9.3**
19	Cyclopentaneundecanoic acid methyl ester	-8.6	-9	-8.8

Journal of Chemical Health Risks
www.jchr.org
JCHR (2026) 16(3), 312-331 | ISSN:2251-6727

20	Phytol	**-9.2**	**-9.6**	**-9.4**
21	Squalene	**-9.4**	**-9.8**	**-9.6**
22	Docosanoic acid ethyl ester	**-8.8**	**-9.2**	**-9**
23	E-10-Pentadecenol	-8.5	-8.9	-8.7
24	3,7,11,15-Tetramethyl-2-hexadecene-1-ol	-9	-9.4	-9.2
25	Urs-12-en-24-oic acid, 3-oxo, methyl ester	**-9.6**	**-10**	**-9.8**
26	Celecoxib (standard reference)	**-8.5**	**-**	-
27	Infliximab (standard reference)	-	-8	-
28	Tocilizumab (standard reference)	-	-	-8.2